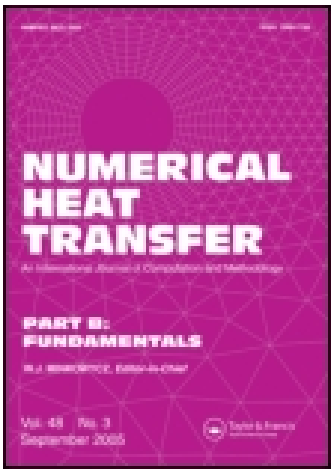

Numerical Heat Transfer, Part B: Fundamentals: An International Journal of Computation and Methodology
Publication details, including instructions for authors and subscription information:
http://www.tandfonline.com/loi/unhb20

Implementation of the Ideal Algorithm on Unsteady Two-Phase Flows and Application Examples

D. L. Sun [a], J. L. Xu [a], P. Ding [b] & W. Q. Tao [c]

[a] State Key Laboratory of Alternate Electrical Power System with Renewable Energy Sources, North China Electric Power University, Beijing, People's Republic of China

[b] College of Storage & Transportation and Architectural Engineering, China University of Petroleum (Hua Dong), Qingdao, ShanDong, People's Republic of China

[c] State Key Laboratory of Multiphase Flow in Power Engineering, School of Energy & Power Engineering, Xi'an Jiaotong University, Xi'an, Shaanxi, People's Republic of China

Published online: 30 Jan 2013.

To cite this article: D. L. Sun, J. L. Xu, P. Ding & W. Q. Tao (2013) Implementation of the Ideal Algorithm on Unsteady Two-Phase Flows and Application Examples, Numerical Heat Transfer, Part B: Fundamentals: An International Journal of Computation and Methodology, 63:3, 204-221, DOI: 10.1080/10407790.2013.751255

To link to this article: http://dx.doi.org/10.1080/10407790.2013.751255

Numerical Heat Transfer, Part B, 63: 204–221, 2013

ISSN: 1040-7790 print/1521-0626 online
DOI: 10.1080/10407790.2013.751255

Taylor & Francis
Taylor & Francis Group

IMPLEMENTATION OF THE IDEAL ALGORITHM ON UNSTEADY TWO-PHASE FLOWS AND APPLICATION EXAMPLES

D. L. Sun[1], J. L. Xu[1], P. Ding[2], and W. Q. Tao[3]

[1]*State Key Laboratory of Alternate Electrical Power System with Renewable Energy Sources, North China Electric Power University, Beijing, People's Republic of China*

[2]*College of Storage & Transportation and Architectural Engineering, China University of Petroleum (Hua Dong), Qingdao, ShanDong, People's Republic of China*

[3]*State Key Laboratory of Multiphase Flow in Power Engineering, School of Energy & Power Engineering, Xi'an Jiaotong University, Xi'an, Shaanxi, People's Republic of China*

For unsteady two-phase flows, the most widely used numerical approaches for coupled solution of continuity and momentum equations are fractional-step methods and SIMPLE-family algorithms. Fractional-step methods have advantages in their fast convergence rates, while their disadvantages lie in conditional stability for initial-value problems. SIMPLE-family algorithms are absolutely stable; however, their convergence rates are slow. To overcome the shortcoming of traditional SIMPLE-family algorithms the, IDEAL algorithm is proposed by the present authors. It is concluded that the IDEAL algorithm overcomes the shortcoming of traditional SIMPLE-family algorithms, thus possessing two advantages of fast convergence rate and absolute stability simultaneously.

1. INTRODUCTION

For unsteady two-phase flows, the main numerical solution methods include particle trajectory models, two-fluid models, and interface-tracking methods. Among these methods, the interface-tracking methods can most accurately reflect the interface information. And the volume-of-fluid (VOF) [1,2] and level set (LS) methods [3–5] are the most widely used interface-tracking methods in the literature. In 2010 a coupled volume-of-fluid and level-set (VOSET) method was proposal by the

Received 29 September 2012; accepted 3 November 2012.

This work was supported by the Young Scientists Fund of the National Natural Science Foundation of China (51106049), the National Basic Research Program of China (2011CB710703), the Beijing Natural Science Foundation (3112022), the Hebei Natural Science Foundation (E2011502057), the Fundamental Research Funds for the Central Universities (12MS44), and the Young Scientists Fund of the National Natural Science Foundation of China (51006121).

Address correspondence to J. L. Xu, State Key Laboratory of Alternate Electrical Power System with Renewable Energy Sources, North China Electric Power University, Beijing 102206, People's Republic of China. E-mail: xjl@ncepu.edu.cn

NOMENCLATURE

C	volume fraction
Co	Courant number
d	initial bubble diameter, m
Eo	Eotvos number
F_{sv}	surface tension force, N/m^3
$\vec{g}$	gravity acceleration, m/s^2
H	smoothed Heaviside function
M	Morton number
p	pressure, Pa
Rs_{Mass}	mass residual
$\vec{u}$	velocity, m/s
γ	density ratio
δt	time interval, s
Δ	grid size, m
ε	width of transition region used for smoothening, m
η	dynamic viscosity, Pa s
κ	interface curvature, 1/m
ρ	density, kg/m^3
σ	surface tension coefficient, N/m
φ	viscosity ratio
ϕ	signed distance function, m

Subscripts

g	gas phase
l	liquid phase
ε	width of transition region used for smoothening

Superscripts

n	current time level
$n+1$	next time level

present authors [6] and later extended to phase-change heat transfer simulation [7], which combines the advantages and overcomes the disadvantages of VOF and LS methods. Therefore, the following research is based on the VOSET method.

For the unsteady two-phase flows studied in this article, on one hand, the VOSET method is adopted to capture the phase interface; on the other hand, the continuity and momentum equations have to be solved jointly. At present, the most widely used numerical approaches for coupled solution of the continuity and momentum equations are fractional-step methods [8–13] and SIMPLE-family algorithms [14–20]. The fractional-step methods have advantages in their fast convergence rates, while their disadvantages lie in conditional stability for initial-value problems due to their explicit or semi-implicit schemes [21]. The SIMPLE-family algorithms are absolutely stable for initial-value problems due to their implicit schemes [21]; however, their convergence rates are slow. On the basis of the above analyses to the fractional step methods and the SIMPLE-family algorithms, it can be seen that they have complementary advantages and disadvantages, so it is an inevitable trend to develop a method combining their advantages.

Recently the present authors proposed an efficient segregated algorithm called IDEAL (inner doubly iterative efficient algorithm for linked equations) [22–25]. In this algorithm there exist inner doubly iterative processes for the pressure equation at each iteration level, which almost completely overcome two approximations in SIMPLE algorithms. Thus, the coupling between velocity and pressure is fully guaranteed, greatly enhancing the convergence rate and stability of the solution process. Therefore, the IDEAL algorithm is adopted to solve the unsteady two-phase flow problems in this article. The IDEAL algorithm is the same as the traditional SIMPLE-family algorithms in terms of absolute stability for initial-value problems. In the following, the analysis will focus on whether the convergence rate of the IDEAL algorithm is much faster than the rates of traditional SIMPLE-family algorithms, further verifying whether the IDEAL algorithm can overcome the disadvantages of the traditional SIMPLE-family algorithms.

As for the solution of algebraic equations formed by discretizing the governing equations, an alternative direction implicit (ADI) method [21] has been widely used in CFD/NHT since the 1980s. The ADI method requires less computing memory but has low solution speed. With the rapid development of the computer industry and CFD/NHT, a more efficient solution method is urgently needed. At present, Krylov subspace methods [26], including Bi-CGSTAB [27,28], GMRES(m) [29], CGS [30], TFQMR [31], QMR [32], and so on, have been the most important iteration techniques for solving algebraic equations, due to their fast solution speeds. All of these methods were compared with each other in [33]. It was found that, among these methods, the Bi-CGSTAB method is much more stable and more efficient. Therefore, the Bi-CGSTAB method is used instead of the traditional ADI method to solve the algebraic equations to further improve the convergence rate of the IDEAL algorithm. To verify the superiority of the IDEAL+Bi-CGSTAB method, three different methods, SIMPLER+ADI, IDEAL+ADI, and IDEAL+Bi-CGSTAB, are compared and analyzed in this article. Here, SIMPLER [34] is a typical SIMPLE-family algorithm.

In the following, the governing equations are described first, and the major solution procedures are briefly reviewed. Then the comparison conditions and the convergence criterion are described, followed by a systemic comparison of the convergence rate of three different methods. Finally, some conclusions are drawn.

2. GOVERNING EQUATIONS

For unsteady laminar incompressible two-phase flows, the interface-tracking method just requires a set of governing equations over the whole domain. In the following, we will give the temporal discretization forms of the governing equations directly.

The temporal discretization form of the volume fraction equation is expressed as

$$\frac{C^{n+1}-C^n}{\delta t}+\nabla\cdot(\vec{u}^n C^n)=0 \tag{1}$$

where n and $n+1$ refer to the current time level and the next time level, respectively.

The temporal discretization forms of the continuity and momentum equations are written as

$$\nabla\cdot\vec{u}^{n+1}=0 \tag{2}$$

$$\begin{aligned}\frac{\vec{u}^{n+1}-\vec{u}^n}{\delta t}+\vec{u}^{n+1}\nabla\cdot(\vec{u}^{n+1})&=\frac{1}{\rho_\varepsilon(\phi^{n+1})}\{-\nabla p^{n+1}\\&+\nabla\cdot\eta_\varepsilon(\phi^{n+1})[(\nabla\vec{u}^{n+1})+(\nabla\vec{u}^{n+1})^{\mathrm{T}}]+\rho_\varepsilon(\phi^{n+1})\vec{g}+F_{sv}^{n+1}\}\end{aligned} \tag{3}$$

The density, viscosity, and surface tension force in Eq. (3) are calculated by the signed distance function ϕ and expressed as

$$\rho_\varepsilon(\phi^{n+1})=\rho_g\left[1-H_\varepsilon(\phi^{n+1})\right]+\rho_l H_\varepsilon(\phi^{n+1}) \tag{4}$$

$$\eta_\varepsilon(\phi^{n+1}) = \eta_g[1 - H_\varepsilon(\phi^{n+1})] + \eta_l H_\varepsilon(\phi^{n+1}) \tag{5}$$

$$F_{sv}^{n+1} = \sigma\kappa(\phi^{n+1})\delta_\varepsilon(\phi^{n+1})\nabla\phi^{n+1} \tag{6}$$

where

$$\kappa(\phi^{n+1}) = \left(\nabla \cdot \frac{\nabla\phi^{n+1}}{|\nabla\phi^{n+1}|}\right) \tag{7}$$

$$\delta_\varepsilon(\phi^{n+1}) = \frac{dH_\varepsilon(\phi^{n+1})}{d\phi^{n+1}} \tag{8}$$

$$H_\varepsilon(\phi^{n+1}) = \begin{cases} 0 & \text{if} \quad \phi^{n+1} < -\varepsilon \\ \frac{1}{2}\left[1 + \frac{\phi^{n+1}}{\varepsilon} - \frac{1}{\pi}\sin\left(\frac{\pi\phi^{n+1}}{\varepsilon}\right)\right] & \text{if} \quad -\varepsilon \le |\phi^{n+1}| \le \varepsilon \\ 1 & \text{if} \quad \phi^{n+1} > \varepsilon \end{cases} \tag{9}$$

In Eq. (9), ε denotes the width of transition region used for smoothening and equals 1.5δ, where δrepresents the grid size.

3. SOLUTION PROCEDURE

For the unsteady two-phase flows studied in this article, on one hand, the VOSET method is used to capture the phase interface and calculate the density, viscosity, and surface tension force; on the other hand, three different methods, SIMPLER+ADI, IDEAL+ADI, and IDEAL+Bi-CGSTAB, are adopted for the coupled solution of the continuity and momentum equations. The brief solution procedures are described as follows.

Step 1. Solve Eq. (1) by the PLIC method to obtain the volume fraction C^{n+1}.
Step 2. Based on C^{n+1}, calculate the signed distance function ϕ^{n+1} near the interfaces by the iterative geometric operation.
Step 3. Based on ϕ^{n+1}, calculate the density $\rho_\varepsilon(\phi^{n+1})$, viscosity $\eta_\varepsilon(\phi^{n+1})$, and surface tension force F_{sv}^{n+1} according to Eqs. (4), (5), and (6).
Step 4. Use three different methods, SIMPLER+ADI, IDEAL+ADI, and IDEAL+Bi-CGSTAB to solve Eqs. (2) and (3), and then obtain the velocity $\vec{u}^{n+1}$.
Step 5. Regard C^{n+1} and $\vec{u}^{n+1}$ as C^n and $\vec{u}^n$, then return to Step 1.
Repeat Steps 1–5 until the time reaches the preset value.

In Steps 1–3, we adopt the VOSET method to capture the interface and calculate the density, viscosity, and surface intension, and this method has been introduced in detail in [6]. In Step 4, the detailed solution procedures of SIMPLER, IDEAL, ADI, and Bi-CGSTAB have been respectively introduced in [34], [35], [21], and [28].

4. COMPARISON CONDITIONS AND CONVERGENCE CRITERION

In order to perform effective comparisons among SIMPLER+ADI, IDEAL+ADI, and IDEAL+Bi-CGSTAB, comparison conditions and convergence criteria should be specified, which are described as follows.

1. **Hardware and codes.** All the calculations are performed on the computer of CPU 2.53 GHz and RAM 1.92 GB along with FORTRAN 77 compiler. For comparison, the codes of the SIMPLER+ADI, IDEAL+ADI, and IDEAL+Bi-CGSTAB methods are compiled under the same program structure. In order to reduce the truncated errors, double-precision digital is adopted to implement computation in our codes.
2. **Discretization scheme.** In order to guarantee the stability and accuracy of numerical solutions, the MUSCL scheme [36] is adopted for the convection term in Eq. (3), which is at least of second-order accuracy and absolutely stable. And the deferred-correction method is adopted to further ensure the stability of computations.
3. **Underrelaxation factor.** In the simulation process of unsteady two-phase flows, the time-step size is very small, and the velocities and pressures at the adjacent time levels change just a little, so the solution process is stable compared with the steady flows. For this reason, the underrelaxation factors for velocity and pressure are all set to be unity.
4. **Inner iteration times.** In the IDEAL algorithm, the first inner iteration times N1 and the second inner iteration times N2 are set as 4 and 4 in this article.
5. **Time step.** The Courant number (Co) is defined by Eq. (10) as

$$\mathrm{Co} = \frac{\delta t}{\Delta/|\vec{u}|} \tag{10}$$

where Δ is the grid size and $|\vec{u}|$ is the absolute value of velocity. A maximum Courant number of 0.1 is set in the present calculation, and a variable time step δt is used based on the fixed Courant number of 0.1.
6. **Convergence criterion.** The maximum mass residual and the maximum u,v-component momentum residuals are all set to be less than 10^{-13}.

5. NUMERICAL COMPARIONS AND ANALYSES

In the following sections, the convergence rates of SIMPLER+ADI, IDEAL+ADI, and IDEAL+Bi-CGSTAB are compared for four unsteady two-phase-flow problems.

5.1. Problem 1: Single Gas Bubble Rising

A single gas bubble rising in an infinite quiescent liquid was analyzed by Grace [37] using a large amount of experimental data from different investigators. It was concluded that four independent dimensionless parameters determine the single gas bubble rising performance. They are Morton number (M), Eotvos number (Eo), viscosity ratio (ϕ), and density ratio (α), which are defined as

$$M = \frac{g\eta_l^4}{\rho_l \sigma^3} \tag{11}$$

$$\mathrm{Eo} = \frac{gd^2(\rho_l - \rho_g)}{\sigma} \tag{12}$$

$$\phi = \frac{\eta_l}{\eta_g} \tag{13}$$

$$\gamma = \frac{\rho_l}{\rho_g} \tag{14}$$

where the subscripts g and l denote the gas phase, and the liquid phase respectively, and d refers to initial bubble diameter.

Here, the domain size is set as $0.05\,\mathrm{m} \times 0.15\,\mathrm{m}$ and a single gas bubble with diameter 0.01 m is released from the position (0.025 m, 0.02 m). The grid number is 50×150 with free slip boundary condition on the surrounding walls. Three cases are studied: $\mathrm{Eo} = 1.0$ and $M = 0.001$ for case 1, $\mathrm{Eo} = 10.0$ and $M = 0.1$ for case 2,

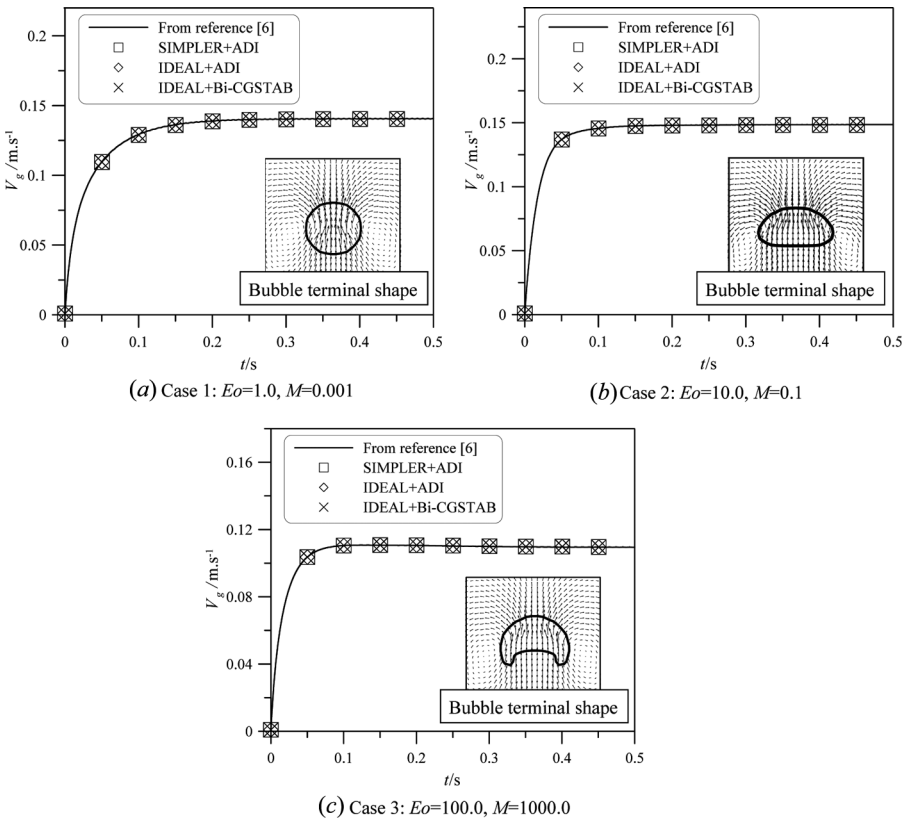

(*a*) Case 1: *Eo*=1.0, *M*=0.001

(*b*) Case 2: *Eo*=10.0, *M*=0.1

(*c*) Case 3: *Eo*=100.0, *M*=1000.0

Figure 1. Rising velocities of single gas bubble with time and bubble terminal shapes.

Eo = 100.0 and $M = 1{,}000.0$ for case 3. In the three cases, both the density ratio α and the viscosity ratio ϕ are equal to 1,000:1.

Figure 1 shows the rising velocities of a single gas bubble with time computed by SIMPLER+ADI, IDEAL+ADI, and IDEAL+Bi-CGSTAB as well as the velocities cited from [6]. It also shows the bubble terminal shapes calculated by IDEAL+Bi-CGSTAB. As shown in this figure, the results calculated by the three different methods are in excellent agreement with those reported in [6]. Those comparisons give some support to the reliability of these methods and the developed codes.

Figure 2 shows the convergence histories of SIMPLER+ADI, IDEAL+ADI, and IDEAL+Bi-CGSTAB under the same iteration number for case 1. Because the momentum residual has the same convergence history as the mass residual, for convenience, this figure just gives the variation curve of the mass residual. To complete one time-level calculation, SIMPLER+ADI requires 130 iterations during which IDEAL+ADI can finish 7 time-level calculations. IDEAL+Bi-CGSTAB performs better than IDEAL+ADI; as shown here, it can finish about 12 time-level calculations, i.e., it requires only about 11 iterations at each time level, verifying its superiority.

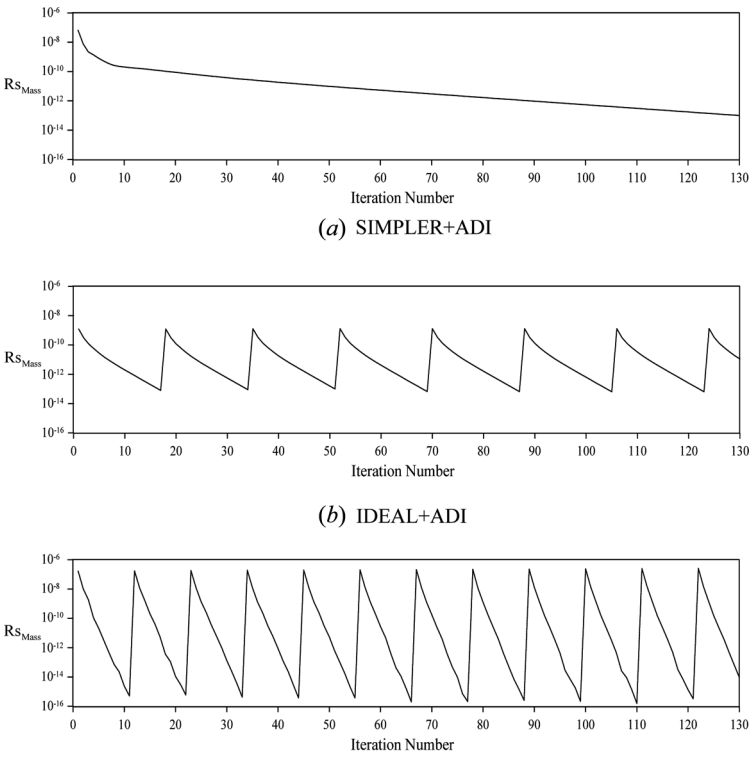

(*a*) SIMPLER+ADI

(*b*) IDEAL+ADI

(*c*) IDEAL+Bi-CGSTAB

Figure 2. Convergence histories of three different methods for case 1 of Problem 1.

Table 1. Computation times of three different methods for Problem 1

	SIMPLER+ADI	IDEAL+ADI	IDEAL+Bi-CGSTAB
Case 1	12,448 s	2,800 s	1,969 s
Case 2	12,260 s	2,465 s	1,574 s
Case 3	11,909 s	2,508 s	1,675 s

Table 2. Reducing ratio of computation time for Problem 1

	Reducing ratio of IDEAL+ADI over SIMPLER+ADI	Reducing ratio of IDEAL+Bi-CGSTAB over IDEAL+ADI	Reducing ratio of IDEAL+Bi-CGSTAB over SIMPLER+ADI
Case 1	77.5%	29.7%	84.2%
Case 2	79.9%	36.1%	87.2%
Case 3	78.9%	33.2%	85.9%

For three different cases of Problem 1, Tables 1 and 2 show the computation times and the reducing ratio of computation time, respectively. It is found that the computation time of IDEAL+ADI is 77.5–79.9% shorter than that of SIMPLER+ADI, and the computation time of IDEAL+Bi-CGSTAB is further shorter than that of IDEAL+ADI by 29.7–36.1%. Therefore, the computation time of IDEAL+Bi-CGSTAB is shorter than that of SIMPLER+ADI by 84.2–87.2%, i.e., its convergence rate is enhanced by 6–8 times.

5.2. Problem 2: Rising and Coalescence of Two Coaxial Gas Bubbles in a Quiescent Liquid

The computation domain of this problem is a rectangular region with of size $0.05\,\text{m} \times 0.15\,\text{m}$, which is filled with quiescent liquid. Two coaxial gas bubbles with diameters of 0.01 m are released from positions (0.025 m, 0.02 m) and (0.025 m, 0.035 m) in this region. The grid number is 50×150 with free-slip boundary condition on the surrounding walls. The Eotvos and Morton numbers are equal to 10.0 and 0.1, respectively, and both the density ratio and the viscosity ratio are 1,000:1.

Figure 3 shows the rising and coalescence of these two gas bubbles calculated by IDEAL+Bi-CGSTAB. Due to the relatively small drag force acting on the trailing bubble, its rising velocity is rapid and its shape is slender compared with the leading bubble. From this, the behavior of the trailing bubble is completely different from the leading bubble, in accordance with the bubble dynamics principle.

Figure 4 shows the convergence histories of SIMPLER+ADI, IDEAL+ADI, and IDEAL+Bi-CGSTAB under the same iteration number for Problem 2. SIMPLER+ADI requires 156 iterations to complete one time-level calculation; IDEAL+ADI can complete about 7 time-level calculations under the same iteration number; IDEAL+Bi-CGSTAB can accomplish about 17 time-level calculations, i.e., it requires only about 9 iterations at each time level.

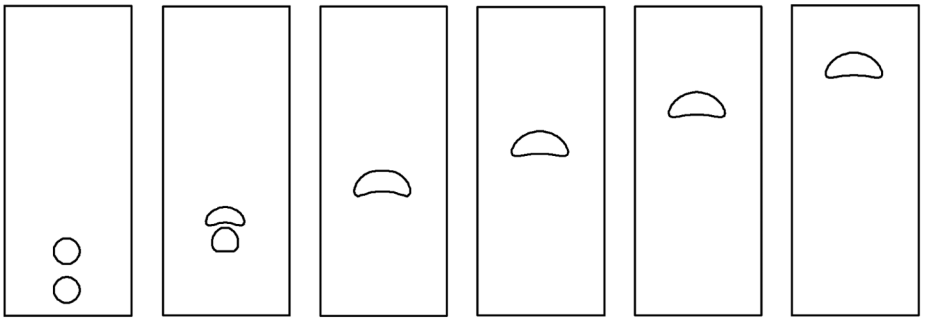

Figure 3. Rising and coalescence of two coaxial gas bubbles in a quiescent liquid.

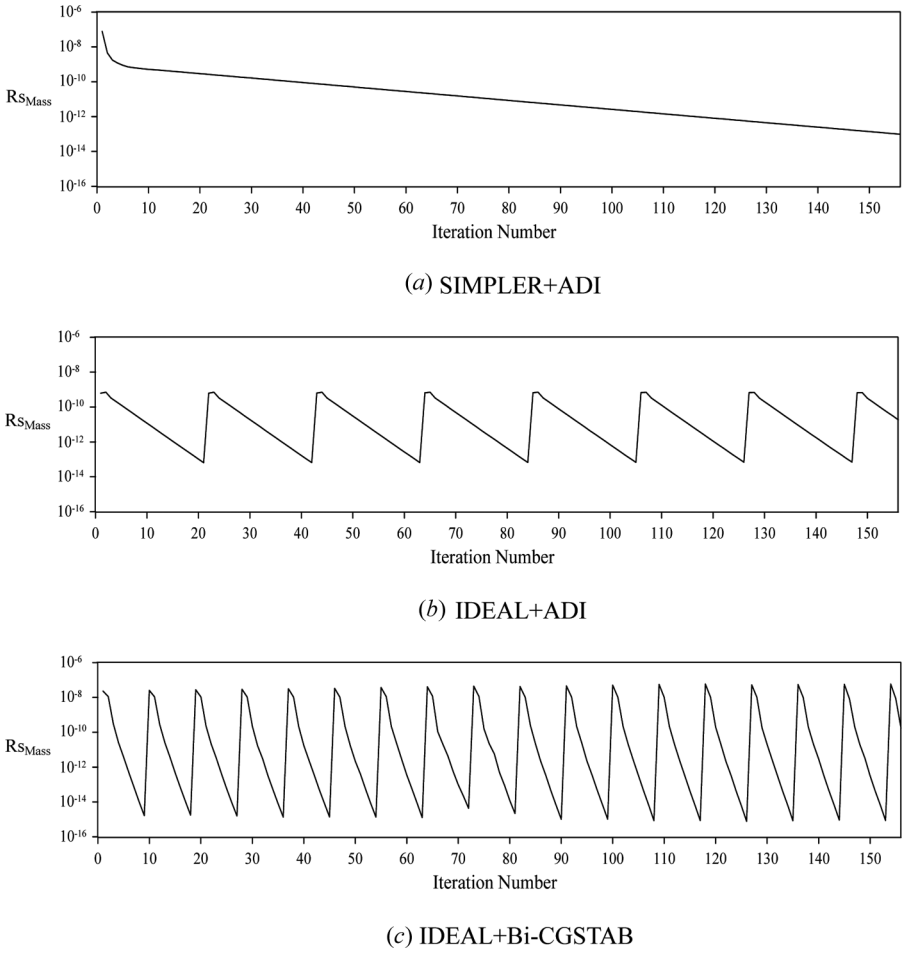

Figure 4. Convergence histories of three different methods for Problem 2.

Table 3. Computation times of three different methods for Problem 2

SIMPLER+ADI	IDEAL+ADI	IDEAL+Bi-CGSTAB
12,196 s	2,936 s	1,924 s

Table 4. Reducing ratio of computation time for Problem 2

Reducing ratio of IDEAL+ADI over SIMPLER+ADI	Reducing ratio of IDEAL+Bi-CGSTAB over IDEAL+ADI	Reducing ratio of IDEAL+Bi-CGSTAB over SIMPLER+ADI
75.9%	34.5%	84.2%

Tables 3 and 4 show, respectively, the computation times and corresponding reducing ratios for Problem 2. For IDEAL+ADI, the reducing ratio of computation time is 75.9% over SIMPLER+ADI. The convergence performance of IDEAL+Bi-CGSTAB is further improved, and its computation time is shorter than that of IDEAL+ADI by 34.5%. Therefore, the computation time of IDEAL+Bi-CGSTAB is shorter than that of SIMPLER+ADI by 84.2%, i.e., its convergence rate is enhanced by 6 times.

5.3. Problem 3: Droplet Falling and Collicting with Quiescent Liquid

The computation domain of this problem is a rectangular region of size $0.03\,\mathrm{m} \times 0.06\,\mathrm{m}$. Its bottom region is filled with quiescent liquid and the top region is filled with quiescent gas. The liquid free-surface height is 0.009 m. A liquid droplet of 0.005 m diameter is released from position (0.015 m, 0.04 m) and experiences two stages, free falling and collision with quiescent liquid. The gas density $\rho_g = 1.205\,\mathrm{kg/m^3}$ and viscosity $\eta_g = 1.81 \times 10^{-5}$ Pa.s. The liquid density $\rho_l = 998.2\,\mathrm{kg/m^3}$ and viscosity $\eta_l = 1.004 \times 10^{-3}$ Pa.s. The gravity $g = 9.8\,\mathrm{m/s^2}$ and surface tension coefficient $\sigma = 0.072\,\mathrm{N/m}$. Calculations are performed for computational grids of 100×200 with free-slip boundary condition on the surrounding walls.

Figure 5 shows two processes: one is the droplet falling process before 0.075 s; the other is the droplet collision process with the quiescent liquid after 0.075 s. Figure 6 shows the theoretical solutions of the droplet falling velocity without gas drag force (i.e., $v = gt$) and the results computed by SIMPLER+ADI, IDEAL+ADI, and IDEAL+Bi-CGSTAB. The calculation results agree very well with the theoretical solutions at the beginning stage. With the advance of time, the calculation results are gradually lower than the theoretical solutions. The reason for this is that the gas drag force is considered in calculation results, while it is neglected in theoretical solutions. To analyze further, because the droplet falling velocity is low and the influence of the gas drag force is small at the beginning stage, the calculation results are consistent with the theoretical solutions. As the gas drag force increases gradually with increase of the droplet falling velocity, the calculation results tend to be lower than the theoretical solutions. From this figure, we can also

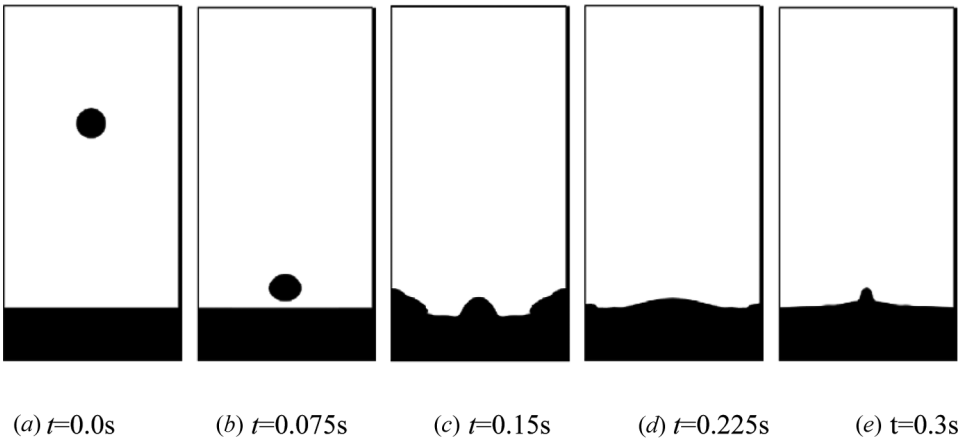

Figure 5. Droplet falling and its collision with quiescent liquid.

see that the results calculated by the three different methods agree with each other very well. All of the above analyses verify the accuracy and feasibility of SIMPLER+ADI, IDEAL+ADI, and IDEAL+Bi-CGSTAB.

Figure 7 shows the convergence histories of SIMPLER+ADI, IDEAL+ADI, and IDEAL+Bi-CGSTAB for Problem 3. SIMPLER+ADI requires 249 iterations to complete one time-level calculation; IDEAL+ADI can complete about 9 time-level calculation under the same iteration number. Significantly, IDEAL+Bi-CGSTAB can accomplish about 32 time-level calculations, i.e., it requires only about 8 iterations at each time level.

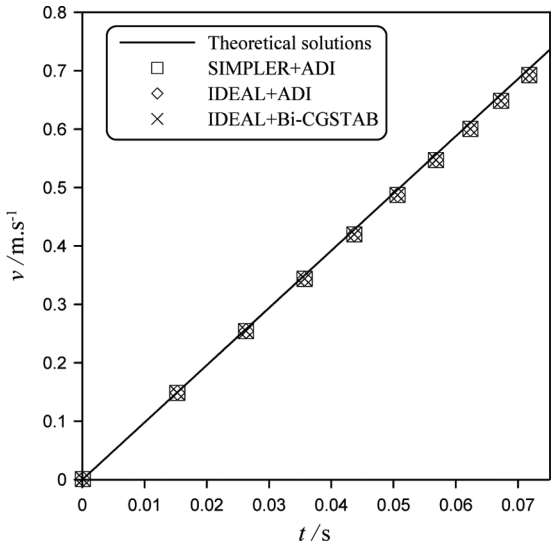

Figure 6. Droplet falling velocity with time before its collision with quiescent liquid.

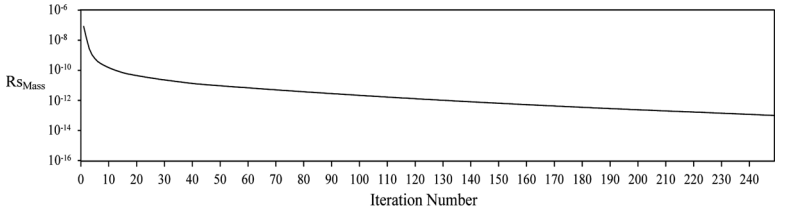

(*a*) SIMPLER+ADI

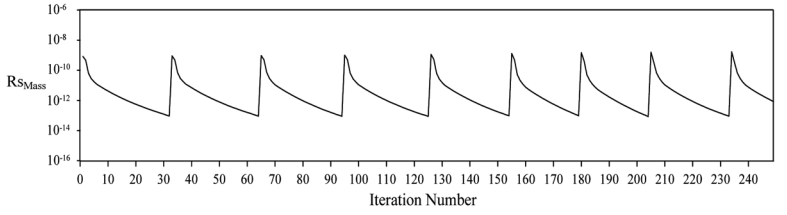

(*b*) IDEAL+ADI

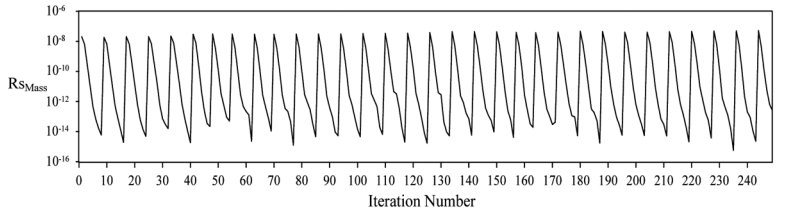

(*c*) IDEAL+Bi-CGSTAB

Figure 7. Convergence histories of three different methods for Problem 3.

Tables 5 and 6 show, respectively, the computation times and reducing ratios for Problem 3. The reducing ratio of computation time of IDEAL+ADI is 66.3% over SIMPLER+ADI, and the convergence performance of IDEAL+Bi-CGSTAB is further improved due to its computation time being much shorter than that of IDEAL+ADI, by 77.7%. So the computation time of IDEAL+Bi-CGSTAB is largely shorter than that of SIMPLER+ADI, by 92.5%, i.e., its convergence rate is enhanced by 13 times.

5.4. Problem 4: Dam Break Problem

Figure 8 shows the physical model of the dam break problem. A liquid column, which has width 0.146 m and height 0.292 m, is stationary in the left side of a vessel

Table 5. Computation times of three different methods for Problem 3

SIMPLER+ADI	IDEAL+ADI	IDEAL+Bi-CGSTAB
89,852 s	30,275 s	6,764 s

Table 6. Reducing ratio of computation time for Problem 3

Reducing ratio of IDEAL+ADI over SIMPLER+ADI	Reducing ratio of IDEAL+Bi-CGSTAB over IDEAL+ADI	Reducing ratio of IDEAL+Bi-CGSTAB over SIMPLER+ADI
66.3%	77.7%	92.5%

at the initial time. The width and height of the vessel are 4 times the width of the initial liquid column. The liquid and background gas physical properties are $\rho_l = 1.0 \times 10^3\,\mathrm{kg/m^3}$, $\mu_l = 0.5\,\mathrm{Pa.s}$, $\rho_g = 1.0\,\mathrm{kg/m^3}$ and $\mu_g = 0.5 \times 10^{-3}\,\mathrm{Pa.s}$. The gravity $g = 9.8\,\mathrm{m/s^2}$ and surface tension coefficient $\sigma = 0.0755\,\mathrm{N/m}$. Calculations are performed for computational grids of 150×150 with free-slip boundary condition.

Figure 9 shows the dam break process calculated by IDEAL+Bi-CGSTAB. The liquid column collapses due to the effect of gravity, and then it flows toward the right side along the ground surface and collides with the right wall at about 0.3 s.

Figure 10 shows the history of fluid front marching along the ground surface. As shown here, the numerical results calculated by SIMPLER+ADI, IDEAL+ADI, and IDEAL+Bi-CGSTAB agree with each other very well, and these results have only about 10% deviation from the experimental data [38]. It also can be found that our simulation results are much closer to the experimental data compared with the numerical results calculated by SOLA-VOF [1].

Figure 11 shows the convergence histories of SIMPLER+ADI, IDEAL+ADI, and IDEAL+Bi-CGSTAB for Problem 4. To complete one time-level calculation, the iteration number of SIMPLER+ADI reaches 1,842 times, during which IDEAL+ADI completes about 10 time-level calculations and IDEAL+Bi-CGSTAB

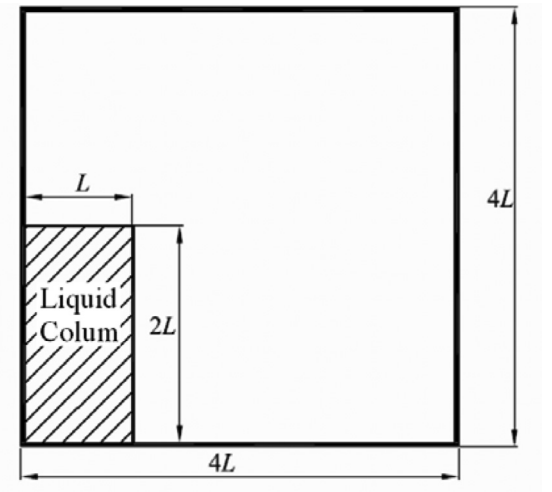

Figure 8. Physical model of dam break problem.

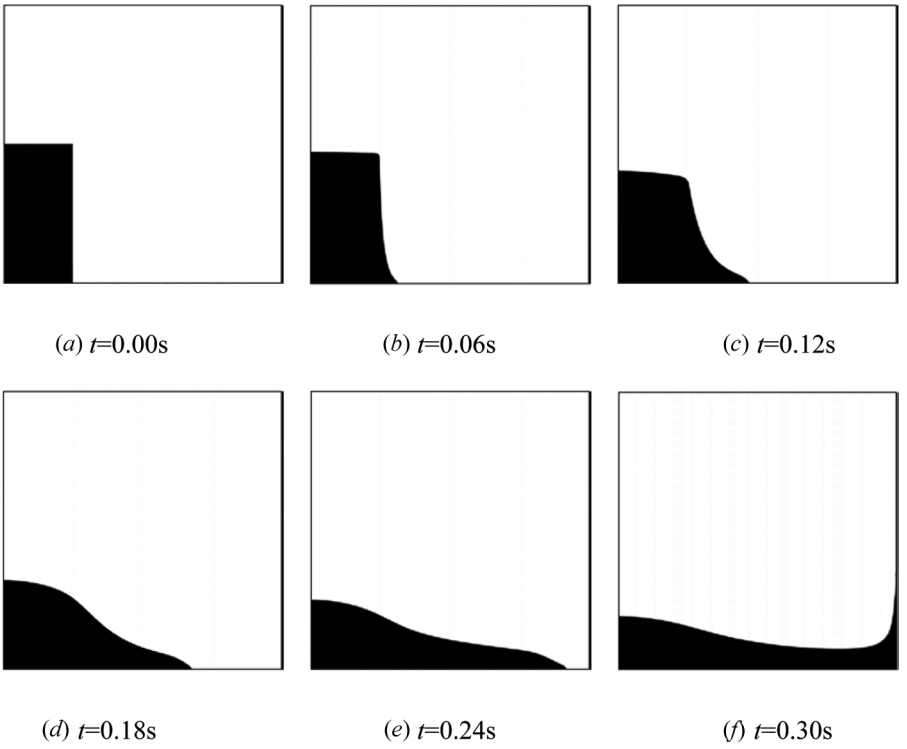

Figure 9. Dam break process.

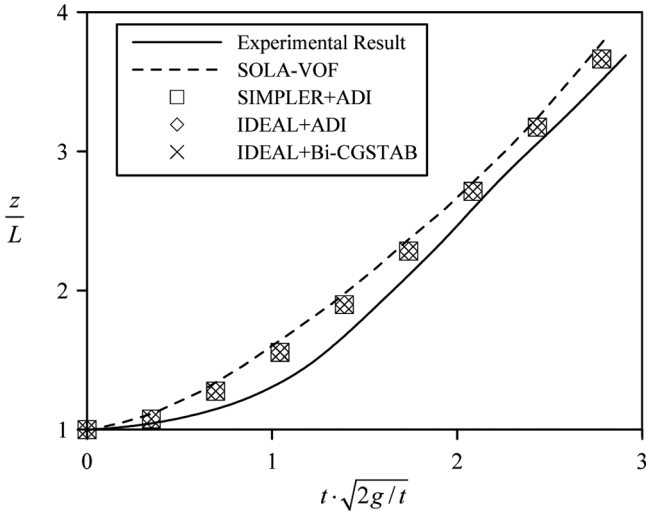

Figure 10. History of fluid front marching along the ground surface.

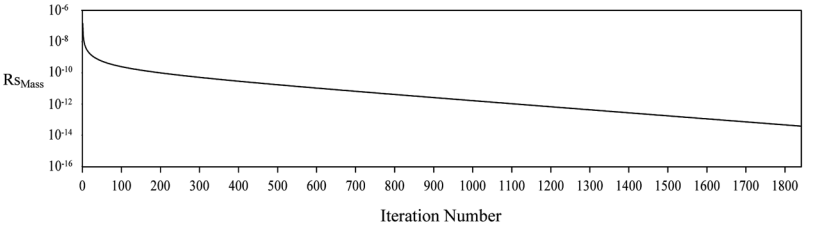

(*a*) SIMPLER+ADI

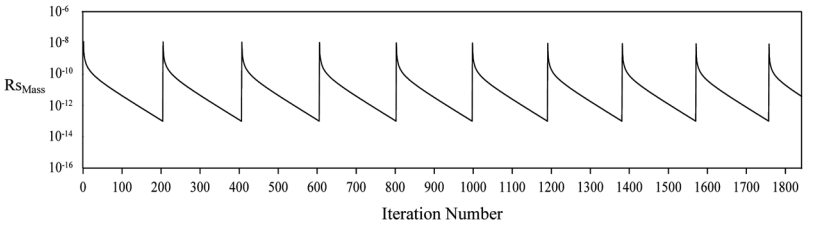

(*b*) IDEAL+ADI

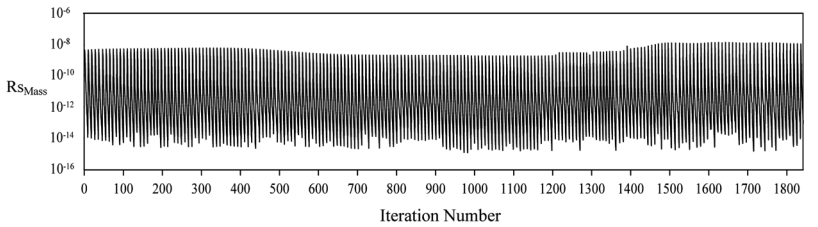

(*c*) IDEAL+Bi-CGSTAB

Figure 11. Convergence histories of three different methods for Problem 4.

completes about 126 time-level calculations. To sum up, the convergence performance of IDEAL+Bi-CGSTAB has been greatly improved, with 9 iterations at each time level.

Tables 7 and 8 show, respectively, the computation times and reducing ratios for Problem 4. The reducing ratio of computation time of IDEAL+ADI is 80.1% over SIMPLER+ADI. And compared with IDEAL+ADI, the computation time of IDEAL+Bi-CGSTAB is further greatly shortened by 94.2%. Finally, the reducing ratio of computation time of IDEAL+Bi-CGSTAB is up to 98.9% over SIMPLER+ADI, i.e., its convergence rate is greatly increased, by 87 times.

Table 7. Computation times of three different methods for Problem 4

SIMPLER+ADI	IDEAL+ADI	IDEAL+Bi-CGSTAB
300,549 s	59,882 s	3,452 s

Table 8. Reducing ratio of computation time for Problem 4

Reducing ratio of IDEAL+ADI over SIMPLER+ADI	Reducing ratio of IDEAL+Bi-CGSTAB over IDEAL+ADI	Reducing ratio of IDEAL+Bi-CGSTAB over SIMPLER+ADI
80.1%	94.2%	98.9%

6. CONCLUSIONS

For the unsteady two-phase flows studied in this article, on one hand, the VOSET method is used to capture the interface and calculate the density, viscosity, and surface tension force; on the other hand, three different methods, SIMPLER+ADI, IDEAL+ADI, and IDEAL+Bi-CGSTAB, are adopted for the coupled solution of the continuity and momentum equations. The convergence rates of the three different methods are compared for four unsteady two-phase-flow problems. The conclusions are summarized as follows.

1. The computation time of IDEAL+ADI is shorter than that of SIMPLER+ADI by 66.3–80.1%.
2. The convergence performance of IDEAL+Bi-CGSTAB is further improved. Its computation time is shortened by 29.7–94.2% compared to IDEAL+ADI.
3. The computation time of IDEAL+Bi-CGSTAB is shortened greatly. Its reducing ratio of computation time over SIMPLER+ADI is as high as 84.2–98.9%, i.e., its convergence rate is greatly improved, by 6–87 times.

To conclude, the above analyses indicate that the IDEAL algorithm overcomes the disadvantage of low convergence rate of the traditional SIMPLE-family algorithms. Therefore, it can be concluded that the IDEAL algorithm possesses two advantages of fast convergence rate and absolute stability simultaneously.

REFERENCES

1. C. W. Hirt and B. D. Nichols, Volume of Fluid (VOF) Method for the Dynamics of Free Boundary, *J. Comput. Phys.*, vol. 39, pp. 201–225, 1981.
2. M. Huang, L. L. Wu, and B. Chen, A Piecewise Linear Interface-Capturing Volume-of-Fluid Method Based on Unstructured Grids, *Numer. Heat Transfer B*, vol. 61, pp. 412–437, 2012.
3. S. Osher and J. A. Sethian, Fronts Propagating with Curvature Dependent Speed: Algorithms Based on Hamilton-Jacobi Formulations, *J. Comput. Phys.*, vol. 79, pp. 12–49, 1988.
4. V. H. Gada and A. Sharma, On Derivation and Physical Interpretation of Level Set Method-Based Equations for Two-Phase Flow Simulations, *Numer. Heat Transfer B*, vol. 56, pp. 307–322, 2009.
5. P. T. Wang, H. W. Sun, P. Y. Wong, H. Fukuda, and T. Ando, Modeling of Droplet-Based Processing for the Production of High-Performance Particulate Materials using the Level Set Method, *Numer. Heat Transfer A*, vol. 61, pp. 401–416, 2012.

6. D. L. Sun and W. Q. Tao, A Coupled Volume-of-Fluid and Level Set (VOSET) Method for Computing Incompressible Two-Phase Flows, *Int. J. Heat Mass Transfer*, vol. 53, pp. 645–655, 2010.
7. D. Z. Guo, D. L. Sun, Z. Y. Li, and W. Q. Tao, Phase Change Heat Transfer Simulation for Boiling Bubbles Arising from a Vapor Film by the VOSET Method, *Numer. Heat Transfer A*, vol. 59, pp. 857–881, 2011.
8. M. Sussman, E. Fatemi, and P. Smereka, An Improved Level Set Method for Incompressible Two-Phase Flows, *J. Comput. Phys.*, vol. 27, pp. 663–680, 1998.
9. T. Kawamura and Y. Kodama, Numerical Simulation Method to Resolve Interactions between Bubbles and Turbulence, *Int. J. Heat Fluid Flow*, vol. 23, pp. 627–638, 2002.
10. M. Van Sint Annaland, N. G. Deen, and J. A. M. Kuipers, Numerical Simulation of Gas Bubbles Behaviour Using a Three-Dimensional Volume of Fluid Method, *Chem. Eng. Sci.*, vol. 60, pp. 2999–3011, 2005.
11. X. Z. Zhao, C. H. Hu, and Z. C. Sun, Numerical Simulation of Extreme Wave Generation Using VOF Method, *J. Hydrodyn.*, vol. 22, pp. 466–477, 2010.
12. V. H. Gada and A. Sharma, On a Novel Dual-Grid Level-Set Method for Two-Phase Flow Simulation, *Numer. Heat Transfer B*, vol. 59, pp. 26–57, 2011.
13. D. Datta, V. H. Gada, and A. Sharma, Analytical and Level-Set Method-Based Numerical Study for Two-Phase Stratified Flow in a Plane Channel and a Square Duct, *Numer. Heat Transfer, A*, vol. 60, pp. 347–380, 2011.
14. R. Banerjee, A Numerical Study of Combined Heat and Mass Transfer in an Inclined Channel Using the VOF Multiphase Model, *Numer. Heat Transfer A*, vol. 52, pp. 163–183, 2007.
15. M. H. Yuan, Y. H. Yang, and T. S. Li, Numerical Simulation of Film Boiling on a Sphere with a Volume of Fluid Interface Tracking Method, *Int. J. Heat Mass Transfer*, vol. 51, pp. 1646–1657, 2008.
16. B. Wang, H. Q. Zhang, and X. L. Wang, A Time-Series Stochastic Separated Flow (TSSSF) Model for Turbulent Two-Phase Flows, *Numer. Heat Transfer B*, vol. 55, pp. 73–90, 2009.
17. J. A. Ramirez and C. Cortes, Comparison of Different URANS Schemes for the Simulation of Complex Swirling Flows, *Numer. Heat Transfer B*, vol. 58, pp. 98–120, 2010.
18. N. Nikolopoulos and G. Bergeles, The Effect of Gas and Liquid Properties and Droplet Size Ratio on the Central Collision between Two Unequal-Size Droplets in the Reflexive Regime, *Int. J. Heat Mass Transfer*, vol. 54, pp. 678–691, 2011.
19. A. Hassanvand and S. H. Hashemabadi, Direct Numerical Simulation of Mass Transfer from Taylor Bubble Flow through a Circular Capillary, *Int. J. Heat Mass Transfer*, vol. 55, pp. 5959–5971, 2012.
20. L. Bu, J. Y. Zhao, and K. J. Tseng, Study on Momentum Interpolation Methods with Curvilinear Collocated Grids in Single-Phase and Two-Phase Flows, *Numer. Heat Transfer B*, vol. 61, pp. 298–310, 2012.
21. W. Q. Tao, *Numerical Heat Transfer*, 2nd ed., Xi'an Jiaotong University Press, Xi'an, China, 2001.
22. D. L. Sun, Z. G. Qu, Y. L. He, and W. Q. Tao, An Efficient Segregated Algorithm for Incompressible Fluid Flow and Heat Transfer Problems—IDEAL (Inner Doubly Iterative Efficient Algorithm for Linked Equations) Part I: Mathematical Formulation and Solution Procedure, *Numer. Heat Transfer B*, vol. 53, pp. 1–17, 2008.
23. D. L. Sun, Z. G. Qu, Y. L. He, and W. Q. Tao, An Efficient Segregated Algorithm for Incompressible Fluid Flow and Heat Transfer Problems—IDEAL (Inner Doubly Iterative Efficient Algorithm for Linked Equations) Part II: Application Examples, *Numer. Heat Transfer B*, vol. 53, pp. 18–38, 2008.

24. D. L. Sun, W. Q. Tao, J. L. Xu, and Z. G. Qu, Implementation of IDEAL Algorithm on Nonorthogonal Curvilinear Coordinates for Solution of 3-D Incompressible Fluid Flow and Heat Transfer Problems, *Numer. Heat Transfer B*, vol. 59, pp. 147–168, 2011.
25. D. L. Sun, Q. P. Liu, J. L. Xu, and W. Q. Tao, Effects of Inner Iteration Times on the Performance of IDEAL Algorithm, *Int. Commun. Heat Mass Transfer*, vol. 38, pp. 1195–1200, 2011.
26. Y. Saad, *Iterative Methods for Sparse Linear Systems*, PWS Publishing, New York, 1996.
27. H. A. Van Der Vorst, BI-CGSTAB: A Fast and Smoothly Converging Variant of BI-CG for the Solution of Nonsymmetric Linear Systems, *SIAM J. Sci. Stat. Comput.*, vol. 13, pp. 631–644, 1992.
28. D. L. Sun, Y. P. Yang, J. L. Xu, and W. Q. Tao, Performance Analysis of IDEAL Algorithm Combined with Bi-CGSTAB Method, *Numer. Heat Transfer B*, vol. 56, pp. 411–431, 2010.
29. S. Vakili and M. Darbandi, Recommendations on Enhancing the Efficiency of Algebraic Multigrid Preconditioned GMRES in Solving Coupled Fluid Flow Equations, *Numer. Heat Transfer B*, vol. 55, pp. 232–256, 2009.
30. J. B. Zhao and Z. H. Sheng, An Improved Conjugate Gradient Square Algorithm, *J. Southeast Univ. (Nat. Sci. Ed.)*, vol. 29, pp. 43–48, 1999.
31. R. W. Freund, A Transpose-Free Quasi-minimal Residual Algorithm for Non-Hermitian Linear Systems, *SIAM J. Sci. Stat. Comput.*, vol. 14, pp. 470–482, 1993.
32. R. W. Freund and N. M. Nachtigal, An Implementation of the QMR Method Based on Coupled Two-Term Recurrences, *SIAM J. Sci. Stat. Comput.*, vol. 15, pp. 313–337, 1994.
33. W. W. Jin, D. L. Sun, W. Q. Tao, and Y. L. He, Analysis of Solution Characteristic for Krylov Subspace Methods in SIMPLER Algorithm, *J. Eng. Thermophys.*, vol. 28, pp. 478–480, 2007.
34. S. V. Patankar, A Calculation Procedure for Two-Dimensional Elliptic Situations, *Numer. Heat Transfer*, vol. 4, pp. 409–425, 1981.
35. D. L. Sun, Z. G. Qu, Y. L. He, and W. Q. Tao, Performance Analysis of IDEAL Algorithm for Three-Dimensional Incompressible Fluid Flow and Heat Transfer Problems, *Int. J. Numer. Meth. Fluids.*, vol. 61, pp. 1132–1160, 2009.
36. B. van Leer, Towards the Ultimate Conservation Difference Scheme. V—A Second-Order Sequel to Godunov's Method, *J. Comput. Phys.*, vol. 23, pp. 101–136, 1977.
37. J. R. Grace, Shapes and Velocities of Bubbles Rising in Infinite Liquids, *Trans. Inst. Chem. Eng.*, vol. 51, pp. 116–120, 1973.
38. J. C. Martin and W. J. Moyce, An Experimental Study of the Collapse of Fluid Columns on a Rigid Horizontal Plane, *Philo. Trans. R. Soc. Lond. A.*, vol. 244, pp. 312–324, 1952.